KSCE Journal of Civil Engineering (2024) 28(4):1253-1266
DOI 10.1007/s12205-024-1309-8

pISSN 1226-7988, eISSN 1976-3808
www.springer.com/12205

Geotechnical Engineering

Influence of Hydraulic Distribution Pattern on the Rock Slope Stability under Block Toppling Failure

Neeraj Chaudhary[a], **Subhadeep Metya**[a], **and Keshav Kumar Sharma**[a]

[a]*Dept. of Civil Engineering, NIT Jamshedpur, Jharkhand 831014, India*

ARTICLE HISTORY

Received 24 June 2023
Accepted 27 November 2023
Published Online 3 February 2024

KEYWORDS

Rock slope stability
Block toppling failure
Hydraulic distribution forms
Ground water pressure
Analytical model

ABSTRACT

In this paper, an analytical model for the stability analysis of rock slope subjected to block toppling pertaining to different hydraulic forms has been developed. In the traditional analytical model, ground water pressure is considered to be varied hydrostatically. To better reflect the physical situation, three different hydraulics forms have been considered in developing a stability model for a rock slope susceptible to block toppling. It is well known fact that presence of ground water causes the instability in a rock slope. The present study observes that hydraulic distribution forms also significantly influence the stability of the rock slope. Ground water pressure markedly increases the toppling forces on the blocks and reduces the normal and shear force at the base of block along failure plane, thereby causing instability. The increase in toppling force and reduction in the factor of safety on the blocks are more prominent when the flow slit is blocked, indicating a condition of permanent or seasonal frozen strata. The study highlights that adopting the traditional hydraulic form to analyse block toppling stability, considering presence of ground water would not be suitable for all field conditions. This necessitates the selection of an appropriate hydraulic distribution form based on the encountered field conditions.

1. Introduction

In hilly terrain, landslides are common geological occurrences. It not only causes destruction of property, injury, and loss of human life but also has detrimental effects on the socio-economic and environmental conditions of the locality. Therefore, slope stability is a serious concern for the continuous development of highways, bridges, dams, steep mine slopes and urban population in mountainous areas. Discontinuity patterns present in the rock mass defines failure mode such as planar, wedge, circular and toppling failure of rock slopes (Goodman and Bray, 1976). Toppling failure is one of the complex failure mechanisms in the rock engineering, and the most common mode of instability in layered rock, involving the rotation of blocks or columns about the base and overturning (Willey, 1980; Zanbak, 1983; Aydan and Kawamoto, 1992; Adhikary et al., 1997; Amini et al., 2017; Sari, 2019). Toppling failures are invariably observed in rock masses comprising a dominating set of discontinuities that strikes parallel to the slope and dips inwards. The most vulnerable rock types to toppling failure are columnar basalts, sedimentary and metamorphic rock with well-developed bedding and foliation planes.

Muller (1968) was the first researcher to specify that rotation of block may have caused the failure of North face of Viont slope. Ashby (1971) was the first, who proposed the name "Toppling" for such instability and proposed toppling stability analysis. Goodman and Bray (1976) classified the toppling failure into two groups namely primary and secondary toppling failure. The weight of the block is the main factor causing instability in primary toppling failure (block, flexure and block-flexure toppling failure) whereas in secondary toppling failure, external factors (natural forces other than weight of block and man-made factors) cause failures. In this study, the analysis presented is intended for the rock slope stability under block-toppling failure.

Block toppling occurs due to the occurrence of two major discontinuity sets: one dips steeply into the slope face and other separates the orthogonal discontinuity defining the height of rock column/block. Shorter rock columns forming the slope toe are forced forward by longer overturning column behind the load. The sliding of these toe blocks enables additional toppling for the

CORRESPONDENCE Subhadeep Metya ✉ smetya.ce@nitjsr.ac.in Dept. of Civil Engineering, NIT Jamshedpur, Jharkhand 831014, India

overall rock slope. Physical models, numerical analysis and analytical approaches are three main tools used to analyse the block toppling stability. Presented study is focused on theoretical analysis using the limit equilibrium approach. Goodman and Bray (1976) were the first authors to develop limit equilibrium approach to analyse rock slope stability under block toppling failure mechanism. This study has been laid as foundation to assess the rock slope stability against block toppling failure. Authors assumed that potentially unstable rock blocks/columns are confined within a discontinuity starting from the topmost rock column, extending to the slope face at an anticipated angle of the weak plane. This stability analysis involves step by step process, in which the dimension of each block and inter-block forces are determined. The stability of all the blocks is then assessed, beginning with the topmost block and ending with the toe block. Each rock block may be stable or fail either by toppling or sliding. The rock slope is considered unstable if toe block fails.

Goodman and Bray's approach was further modified by various researchers. Willey (1980) discussed limitation of Goodman and Bray's analytical approach in the design of slopes subjected to toppling failure and further modified the approach for the use of different friction angles for the sides and along the base. Zanbak (1983) constructed design charts to evaluate support force against toppling using varied slenderness ratio (slope height to block thickness) based on analytical solution. Cruden (1989) further modified it to demonstrate the influence of friction angle through the interface and block base on the stability of rock slope. Bobet (1999) developed an analytical method to assess toppling instability that incorporates the rock mass as a continuous medium instead of a discrete assembly of blocks. Sagaseta and Ca (2001) developed an analytic solution that accounts the infinitesimal thickness of blocks and reported that this technique is appropriate for slopes with higher slenderness ratio (slope height to block thickness). Chen et al. (2005) analysed block toppling failure mode considering connectivity of block base joints. Liu et al. (2008) developed a transfer coefficient method that enables the development of the relationship among the normal forces of the block to analyse the rock slope stability against toppling. Yagoda-Biran and Hatzor (2013) developed a 3D failure mode chart to analyse stability of rock slope with toppling and sliding mode of failure considering a pseudo-static horizontal force passing through centroid simulating seismic force. Zheng et al. (2014) suggested a solution to assess the block toppling stability of rock slope under earthquake with the block slenderness ratio greater than 20. Zhang et al. (2016) investigated the rock toppling mode of failure under earthquake using numerical modelling. Alejano et al. (2018) investigated the effect of weathering in terms of rounding of rock block edges on the stability against block toppling failure using physical modelling and limit equilibrium approach. Azarafza et al. (2021) proposed a fuzzy based toppling instability analysis that can detect and describe toppling occurrence.

It is worth mentioning that presence of ground water has been taken into consideration in some newly developed analytical solution in last decade. Some researchers (Zhao et al., 2015; Wyllie and Mah, 2017; Bowa and Gong, 2021) specified that water present in discontinuities significantly affects block toppling stability. Hoek and Bray (1981) mentioned that the actual hydraulic distribution is not known in rock slope engineering. Furthermore, Tang and Chen (2008) conducted a series of experiments to establish the relationship between pressure distribution and slit of discontinuities under static condition, concluded that complex and specific water pressure distribution forms within discontinuities. In rock slope stability analysis, Hoek and Bray (1981) assumed a hydrostatic water pressure distribution. Many researchers have considered this suggestion for the stability analysis (Tatone and Grasselli, 2010; Zhao et al., 2015; Roy and Maheshwari, 2018; Bowa and Gong, 2021). However, this consideration does not hold true in some field situations, such as in the case of frozen strata over the flow slit and partial blockage at the flow slit (Luo et al., 2010; Zhao et al., 2011). Recent advancements have demonstrated a noteworthy trend towards employing explicit data-driven models to enhance the prediction accuracy of critical hydraulic phenomena (Samadi et al., 2020, 2021; Shafagh Loron et al., 2023).

Keeping the above in view, it may be noted that the effect of water pressure for different flow conditions along failure plane on the stability analysis of rock slope subjected to toppling failure have been overlooked in the literature. In this study, the primary objective is to develop the analytical formulations for the stability analysis of rock-slopes subjected to block-toppling under different hydraulic forms. Based on the literature reviews presented above, three different hydraulics forms have been considered in developing a stability model for a rock slope susceptible to block toppling and this enables a comparative study to be performed for different field situations utilising the developed formulations.

2. Adopted Methodologies

Figure 1 shows an idealised schematic diagram of block toppling on a jointed rock slope. The 2D model comprises rectangular rock blocks/columns with a width of Δx, height of y_n, and unit weigh γ_r, numbered from toe upwards. The dip of the base of block and the dip of orthogonal planes constituting the face of the block are represented by Ψ_p and Ψ_d respectively ($\Psi_d = 90^o - \Psi_p$). The blocks dip into the slope face. resting on a stepped base ascending from one cross joint to the next. The geometries of the jointed slope include the slope height designated as H, slope face angle is designated as Ψ_f, the upper face slope angle designated as Ψ_s and other constants designated as a_1, a_2, and b. The proposed analysis for stability evaluation under various hydraulic forms is focused on idealised geometry. Basic assumptions of the analysis are 1) Each rock block is rigid with sharp rectangular edges. 2) Dip direction of main layers (joints) defining the longitudinal boundary of block must be into the slope. 3) Width and strength characteristics are identical for each block, and blocks are resting over linear failure base plane.

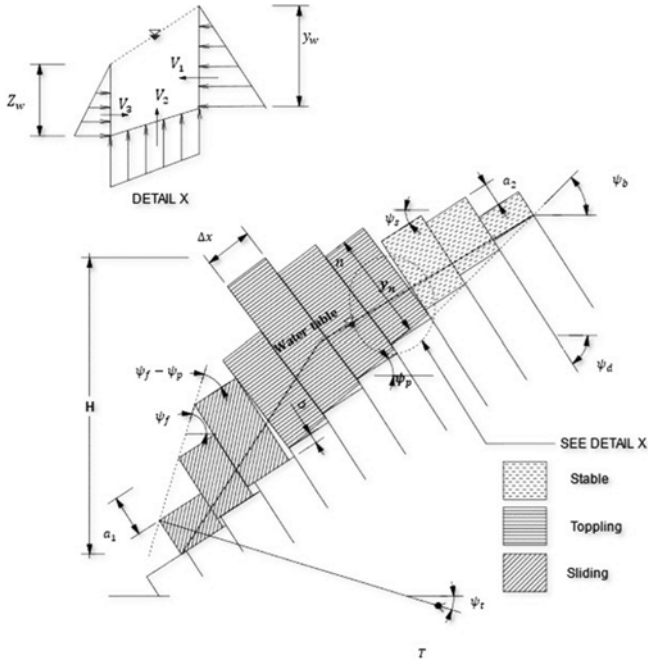

Fig. 1. System for Limit Equilibrium Analysis of Block Toppling on Stepped Base (after Goodman and Bray, 1976)

2.1 Rock Slope Geometry

Primary step in toppling failure mechanism is to compute the dimensions of each rock block. Considering the rectangular block system (Fig. 1), the interface between blocks and base is stepped with an overall dip Ψ_b and may be taken as follows (Goodman and Bray, 1976; Adhikary et al., 1997)

$$\Psi_b \approx (\Psi_p + 10^o) \text{ to } (\Psi_p + 30^o). \quad (1)$$

By resolving slope geometry, the number of blocks n forming the system is given by

$$n = \frac{H}{\Delta x}\left[\text{cosec}\,\Psi_b + \left(\frac{\cot\Psi_b - \cot\Psi_f}{\sin(\Psi_b - \Psi_f)}\right)\sin\Psi_s\right]. \quad (2)$$

2.2 Block Stability

Rock slope stability analysis against block toppling is a two-step process.

2.2.1 Kinematic Analysis of Block Toppling

Prior to main stability analysis i.e., kinetic analysis, kinematic analysis of structural discontinuity is performed in order to determine toppling potential of blocks. If a kinematically unstable condition is observed, the factor of safety is determined using a kinetic analysis utilising the limit equilibrium approach

Considering a single block, toppling occurs when centre of gravity of the block does not lie inside the base and block does not slide across the base. This criterion is represented mathematically as

$$\Psi_p < \phi_p \text{ (Stable against sliding)}, \quad (3)$$

$$\frac{y_n}{\Delta x} < \cot\Psi_p \text{ (Stable against toppling)}, \quad (4)$$

where Ψ_p is the dip of plane forming base of the block, ϕ_p is the friction angle along the base of the block, y_n is the height of nth block and Δx is the width of the block.

While considering series of block, there are two more criteria. The first criterion, discontinuity planes defining the width and base of block should be approximately parallel to the slope face ($\pm$ 20^o), allowing the block toppling without being restrained by the nearby rock deposition. This criterion is represented mathematically as (Wyllie and Mah, 2004)

$$|\alpha_a - \alpha_s| < 20^o \text{ and } |\alpha_b - \alpha_s| < 20^o. \quad (5)$$

where α_a, α_b, and α_s are the dip direction of discontinuities determining base, width and slope face respectively. Another criterion is that interlayer slip may exist across sub-vertical discontinuities determining block width. Considering the in-situ stresses parallel and adjacent to the slope face are uniaxial and, criterion for interlayer slip is written mathematically as (Goodman and Bray, 1976)

$$(90^o - \Psi_b) \le (\Psi_s - \phi_b). \quad (6)$$

2.2.2 Kinetic Analysis of Block Toppling

If kinematic conditions are found to be exist, kinetic stability can be analysed using limit equilibrium approach proposed by Goodman and Bray (1976). This approach consists of three different group of blocks in the manner corresponding to their instability mode: 1) A set of stable rock blocks in the upper portion of slope as these blocks do not satisfy the toppling and sliding criteria (Eqs. (3) and (4)); 2) a set of blocks in intermediate portion of slope, which meet toppling criterion (Eq. (4)); 3) a set of blocks in toe region, those pushed down by the above toppling blocks (Fig. 1). Mode of behaviour of toe block depends on the block and slope geometry, that may be stable, toppling or sliding.

Stability analysis of block toppling is an iterative step wise process that starts with determining the dimension of blocks and inter block forces, and then stability of all the individual block is analysed beginning with the upper block. Fig. 3 is a flow diagram illustrating the procedure to calculate geometry of block and inter-block forces. Considering force and moment equilibrium, each block can be stable, slide or topple. If block topples or slides, a force will be transferred to the next block, by equal in magnitude to the force required to keep the current block in limit equilibrium. The stability of toe block determines the overall slope stability. Slope is considered stable if toe block is stable, conversely, slope is unstable, if toe block is unstable. When the block is subjected to toppling or sliding, frictional forces are developed along the sides and base of the block. Depending on the geological formation, friction angle on base (ϕ_p) and sides (ϕ_d) of block may be different or same. Normally, $\phi_d < \phi_p$ (Wyllie and Mah, 2004; Bowa and Xia, 2018). Fig. 2 depicts all the forces acting on a typical block.

Using limit equilibrium approach, starting from the uppermost block, shear forces generated along the sides of each rock block can be calculated using Eqs. (7) and (8),

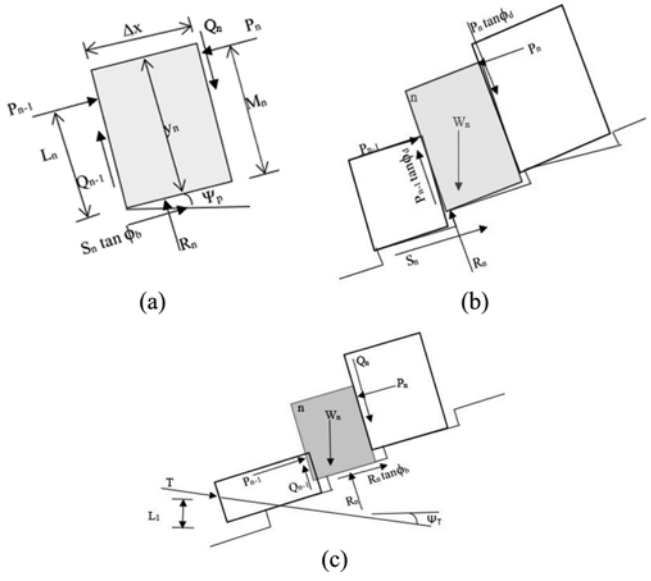

Fig. 2. Limiting Equilibrium Approach for Failure Modes of n^{th} Rock Block, (a) Forces Acting on n^{th} Block, (b) Toppling Failure of n^{th} Block, (c) Sliding Failure of n^{th} Block

$$Q_n = P_n \tan\phi_d , \tag{7}$$

$$Q_{n-1} = P_{n-1} \tan\phi_d . \tag{8}$$

Normal and Shear force acting on the base of block n can be calculated by resolving forces acting on the block,

$$R_n = W_n \cos\Psi_p + (P_n - P_{n-1})\tan\phi_d , \tag{9}$$

$$S_n = W_n \sin\Psi_p + (P_n - P_{n-1}) . \tag{10}$$

Considering rotational equilibrium of block, force $P_{n\text{-}1}$ adequate to prevent toppling (Fig. 2(b))

$$P_{n-1,t} = \frac{P_n(M_n - \Delta x \tan\phi_d) + \left(\frac{W_n}{2}\right)(y_n \sin\Psi_p - \Delta x \cos\Psi_p)}{L_n} . \tag{11}$$

For the block belonging to sliding set (Fig. 2(c))

$$S_n = R_n \tan\phi_p . \tag{12}$$

However, the magnitude of the forces $Q_{n\text{-}1}$, $P_{n\text{-}1}$, and R_n applied to the sides and base of the block, as well as their point of application L_n and M_n are unknown. Even though the problem is indeterminate, the force $P_{n\text{-}1}$ adequate to prevent sliding of block n can be determined if it is assumed that $Q_{n-1} = (P_{n-1}\tan\phi_d)$ then the shear force just adequate to prevent sliding,

$$P_{n-1,s} = P_n - \frac{W_n(\cos\Psi_p \tan\phi_p - \sin\Psi_p)}{(1 - \tan\phi_p \tan\phi_d)} . \tag{13}$$

Toppling force and sliding force is calculated from uppermost block to toe block using Eqs. (11) and (13) respectively. If $P_{n\text{-}1,t}$ is greater than $P_{n\text{-}1,s}$ the block is susceptible to toppling or If $P_{n\text{-}1,s}$ is greater than $P_{n\text{-}1,}$ the block is susceptible to sliding. If both the forces $P_{n\text{-}1,t}$ and $P_{n\text{-}1,s}$ are less than zero, block is said to be stable.

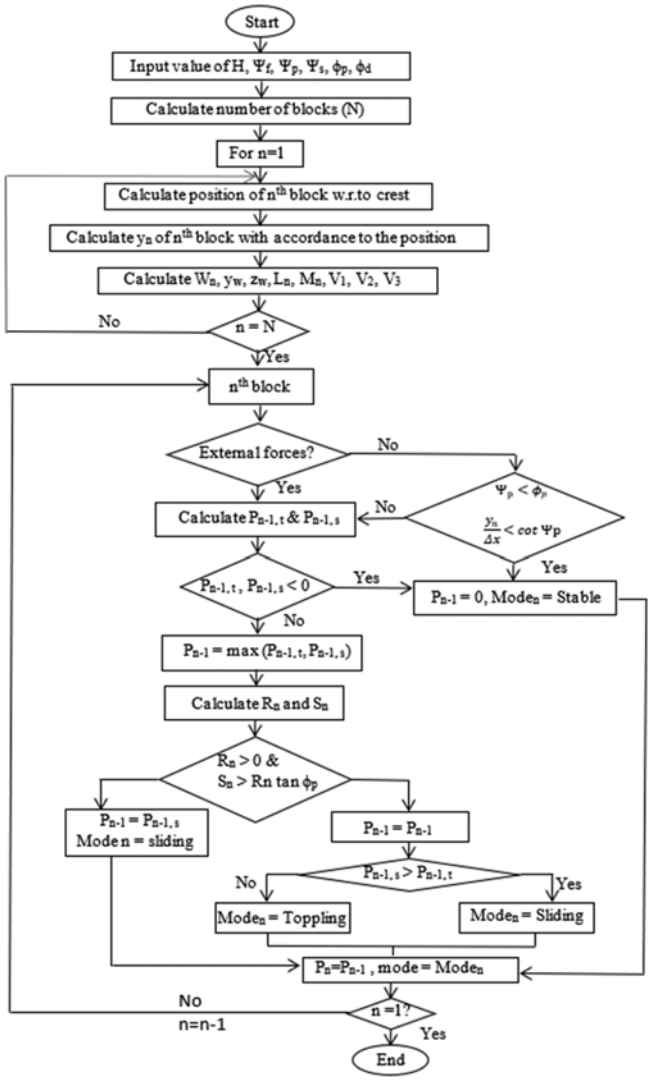

Fig. 3. Flow Diagram for Calculation Procedure of Inter Block Forces and Their Mode of Failure

Force $P_{n\text{-}1}$ can simply be obtained as

$$P_{n-1} = \max(P_{n-1,t}, P_{n-1,s}, 0) . \tag{14}$$

In addition, a check is made if condition $R_n > 0$ & $|S_n| < R_n \tan\phi_p$ is satisfied, sliding does not occur on the base.

2.3 Factor of Safety of Rock Slope Subjected to Block Toppling Failure

The friction angle for limiting equilibrium is required to compute the factor of safety. Firstly, limit equilibrium stability analysis is to be carried out using the actual value of friction angle. If toe block is unstable, then value of friction angles are increased in small increments until the force at toe block P_o is very small (near to zero). Conversely, if toe block is stable, the friction angles are decreased until force at toe block P_o is very small. These values of friction angles are referred to as required friction angles while actual friction angles of the block are referred to as available friction angles. Factor of safety can be calculated as

$$FS = \frac{\tan\phi_{\text{available}}}{\tan\phi_{\text{required}}}. \tag{15}$$

3. Hydraulic Distribution Forms

In field conditions, groundwater may exist that act as an external force to the slope and can affect the stability of rock slope (Wyllie and Mah, 2004; Bowa and Gong, 2021). In case of rock analysis water pressure distribution is complex and cannot be taken as traditional water pressure distribution for all field conditions (Zhao et al., 2015). In this analysis, the external force due to existence of ground water is computed according to the following three field situations:

***Case* 1**: Maximum water pressure at the base of rock block (Fig. 4). ***Case* 2**: Maximum water pressure at the toe of rock slope, as shown in (Fig. 5). ***Case* 3**: Maximum water pressure at the mid distance along base failure plane (Fig. 6).

The practical explanation of the considered three water pressure distribution case are as follows (Shu et al., 2004; Zhao et al., 2011).

Case 1, If degree of slit at failure plane is small. It means, volume of discharged water is less than that of water present in discontinuities. Water pressure may suddenly increase at the bottom of block. This consideration signifies the water pressure distribution diagram similar to conventionally adopted water distribution pattern (Wyllie and Mah, 2004; Roy and Maheshwari, 2018; Bowa and Gong, 2021).

Case 2, At places, where presence of permanently frozen or seasonally frozen strata causes blockage of flow slit. Groundwater can not readily discharge through flow slit at the bottom of failure rock mass, subsequently there will be sharp increase in water pressure at the bottom of failure surface as shown in Fig. 5.

Case 3, If degree of slit at failure plane is large enough so that volume of discharged water is more than that of water present in the discontinuities. The maximum water pressure point along failure plane will gradually vary with time. In this study, water pressure is considered to be maximum at mid distance along the base failure plane.

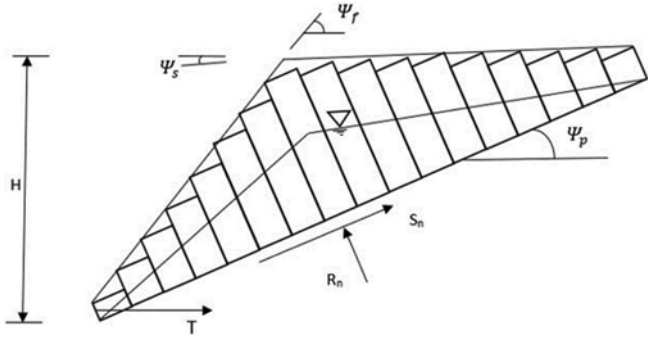

Fig. 4. Rock Slope Subjected to Toppling Failure with Ground Water (Case 1)

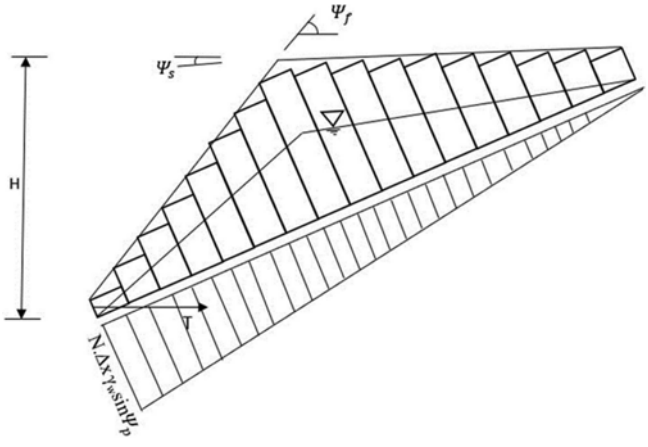

Fig. 5. Rock Slope Subjected to Toppling Failure with Ground Water (Case 2)

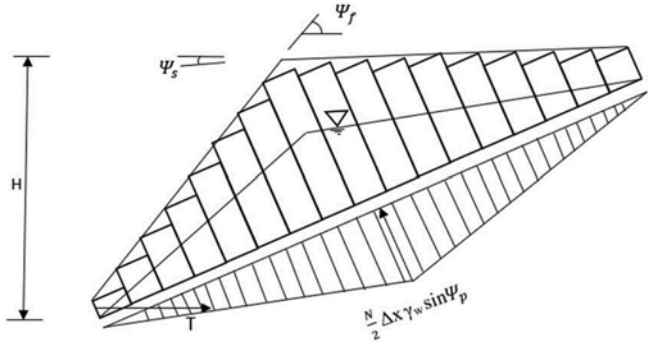

Fig. 6. Rock Slope Subjected to Toppling Failure with Ground Water (Case 3)

4. Analytical Formulations

Figure 7 shows distribution of groundwater forces (V_1, V_2, V_3) and the inter block forces P_n and $P_{n\text{-}1}$ on the nth block of rock slope. Eqs. (9) – (11) are then modified by considering the groundwater forces and resolving all the normal and parallel forces at the base of the blocks using limit equilibrium approach for the considered three different hydraulic distribution forms.

4.1 Case 1: Maximum Water Pressure at the Base of Rock Block

In this case, water pressure is assumed to be distributed as hydrostatically. Symbols used in Fig. 7, γ_w, the water unit weight, y_w and z_w are water depth at upper and downside of block respectively.

Water forces acting on nth block can be expressed as follows

$$V_1 = \frac{1}{2}\gamma_w \cos\Psi_p y_w^2, \tag{16}$$

$$V_2 = \frac{1}{2}\gamma_w \cos\Psi_p (y_w + z_w)\Delta x, \tag{17}$$

$$V_3 = \frac{1}{2}\gamma_w \cos\Psi_p z_w^2. \tag{18}$$

When the rock block is susceptible to toppling failure, then

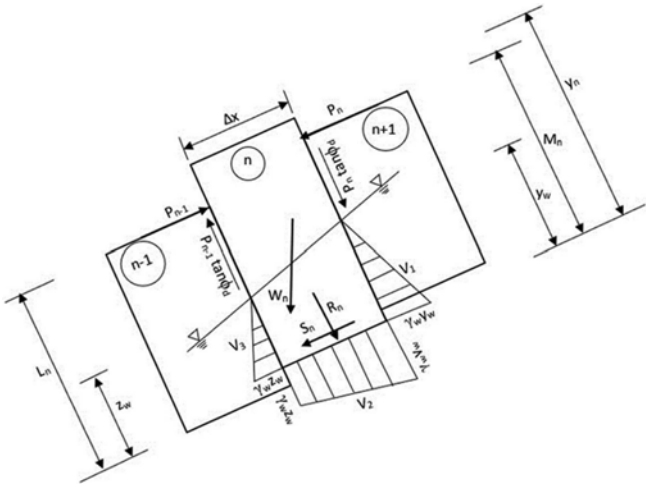

Fig. 7. Water Pressure Distribution at the n[th] Block as per Case 1

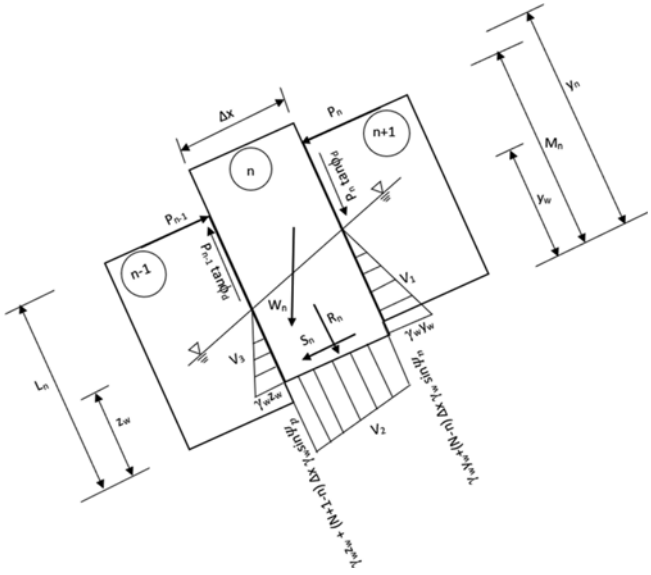

Fig. 8. Water Pressure Distribution at the n[th] Block as Per Case 2

considering rotational equilibrium (Fig. 7), $P_{n\text{-}1,t}$ i.e., force adequate to prevent the rock block against toppling of n[th] block can be determined using Eq. (19).

$$P_n(M_n-\Delta x\tan\phi_d)+\left(\frac{W_n}{2}\right)(y_n\sin\Psi_p-\Delta x\cos\Psi_p)+$$

$$P_{n-1,t}=\frac{V_1\frac{y_w}{3}+\gamma_w\cdot\frac{\Delta x^2}{6}\cos\Psi_p(z_w+2y_w)-V_3\frac{z_w}{3}}{L_n} \quad (19)$$

It is assumed that rock block is in the limit equilibrium state. Force $P_{n\text{-}1,s}$ i.e., adequate to prevent sliding of n[th] block can be calculated as

$$P_{n-1,s}=P_n-\frac{W_n(\cos\Psi_p\tan\phi_p-\sin\Psi_p)-V_1+V_2\tan\phi_p+V_3}{(1-\tan\phi_p\tan\phi_d)}. \quad (20)$$

The normal and shear forces at the rock block base considering ground water under case 1 can be computed as

$$R_n=W_n\cos\Psi_p+(P_n-P_{n-1})\tan\phi_d+(V_1-V_3)\tan\phi_d-V_2\cos\Psi_p, \quad (21)$$

$$S_n=W_n\sin\Psi_p+(P_n-P_{n-1})-(V_1-V_3)-V_2\sin\Psi_p. \quad (22)$$

4.2 Case 2: Maximum Water Pressure at the Toe of Rock Slope

In case of blocked flow slit, water pressure is maximum at toe. The water forces at the n[th] block can be expressed as

$$V_1=\frac{1}{2}\gamma_w\cos\Psi_p y_w^2, \quad (23)$$

$$V_{2,i=(N+1)-n}=\frac{1}{2}\gamma_w\cos\Psi_p(y_w+z_w+(2i-1)\Delta x\sin\Psi_p)\Delta x, \quad (24)$$

$$V_3=\frac{1}{2}\gamma_w\cos\Psi_p z_w^2. \quad (25)$$

Considering rotational equilibrium at n[th] block, $P_{n\text{-}1,t}$ i.e., the force adequate to prevent the rock block against toppling (Fig. 8) can be expressed as

$$P_{n-1,t(i=(N+1)-n)}=$$

$$P_n(M_n-\Delta x\tan\phi_d)+\left(\frac{W_n}{2}\right)(y_n\sin\Psi_p-\Delta x\cos\Psi_p)+V_1\frac{y_w}{3}+$$

$$\frac{\gamma_w\cdot\frac{\Delta x^2}{6}\cos\Psi_p\{z_w+2y_w+(2i-1)\Delta x\sin\Psi_p\}-V_3\frac{z_w}{3}}{L_n}. \quad (26)$$

And sliding force,

$$P_{n-1,s}=P_n-\frac{W_n(\cos\Psi_p\tan\phi_p-\sin\Psi_p)-V_1+V_{2,i}\tan\phi_p+V_3}{(1-\tan\phi_p\tan\phi_d)}. \quad (27)$$

The normal and shear forces at the base of block considering case 2 can be expressed as

$$R_n=W_n\cos\Psi_p+(P_n-P_{n-1})\tan\phi_d+(V_1-V_3)\tan\phi_d-V_{2,i}\cos\Psi_p, \quad (28)$$

$$S_n=W_n\sin\Psi_p+(P_n-P_{n-1})-(V_1-V_3)-V_{2,i}\sin\Psi_p. \quad (29)$$

4.3 Case 3: Maximum Water Pressure at the Mid Distance Along Base Failure Plane

4.3.1 For Top Block to Mid-Block

Toppling force and sliding force can be determined using Eqs. (26) and (27) respectively. Water pressure on the n[th] block that exist between topmost and mid-block is similar to case 2 as shown in Fig. 8.

4.3.2 From to Mid-Block to Toe Block

Figure 9 depicts all the forces acting on n[th] block that exist between middle block and toe block as per case (3) Here, force $P_{n\text{-}1,t}$ i.e., adequate to prevent toppling of n[th] block,

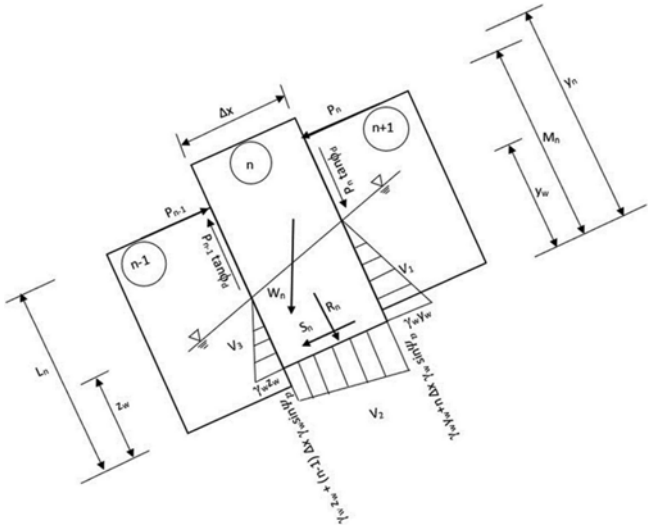

Fig. 9. Water Pressure Distribution on n[th] Block that Exist between the Mid-Block and Toe Block as per Case 3

$$P_{n-1,t} = P_n(M_n - \Delta x\tan\phi_d) + \left(\frac{W_n}{2}\right)(y_n\sin\Psi_p - \Delta x\cos\Psi_p) + V_1\frac{y_w}{3} + \gamma_w\cdot\frac{\Delta x^2}{6}\cos\Psi_p\{z_w + 2y_w + (2n-1)\Delta x\sin\Psi_p\} - V_3\frac{z_w}{3} \Big/ L_n \quad (30)$$

Water forces are as follows

$$V_1 = \frac{1}{2}\gamma_w\cos\Psi_p y_w^2, \quad (31)$$

$$V_{2,n} = \frac{1}{2}\gamma_w\cos\Psi_p(y_w + z_w + (2n-1)\Delta x\sin\Psi_p)\Delta x, \quad (32)$$

$$V_3 = \frac{1}{2}\gamma_w\cos\Psi_p z_w^2. \quad (33)$$

Force i.e., adequate to prevent sliding of block,

$$P_{n-1,s} = P_n - \frac{W_n(\cos\Psi_p\tan\phi_p - \sin\Psi_p) - V_1 + V_{2,n}\tan\phi_p + V_3}{(1-\tan\phi_p\tan\phi_d)}. \quad (34)$$

The normal and shear forces at the base of block considering this case can be expressed as

$$R_n = W_n\cos\Psi_p + (P_n - P_{n-1})\tan\phi_d + (V_1 - V_3)\tan\phi_d - V_{2,n}\cos\Psi_p, \quad (35)$$

$$S_n = W_n\sin\Psi_p + (P_n - P_{n-1}) - (V_1 - V_3) - V_{2,n}\sin\Psi_p. \quad (36)$$

5. Stabilization of Rock Slope by Tensioned Cable

If the toe block shown in Fig. 2(c) is observed to be failed either in toppling or sliding, then overall rock slope is unstable. It is required to stabilize unstable toe block (Wyllie and Mah, 2004) to stabilise the rock slope. To improve the rock slope stability against block toppling failure, reinforcing the toe block using anchors and bolts is conventionally adopted corrective measure. In order to anchor toe block, design parameters are plunge angle of anchor and its distance on toe block from the toe of slope. For the formulation, it is considered to install the anchor at the plunge angle ψ_T and at a distance L_1 above the toe of the slope. To calculate the anchor tension adequate to prevent toppling of toe block (Eqs. (37) – (39)) that incorporates water forces for case (1), (2) and (3) respectively is formulated. Furthermore, Eq. (40) was developed to incorporates water forces and determine anchor tension adequate to prevent sliding of toe block.

$$T_t = \frac{\frac{W_1(y_1\sin\Psi_p - \Delta x\cos\Psi_p)}{2} + P_1(y_1 - \Delta x\tan\phi_d) + V_1\frac{y_w}{3} + \gamma_w\cdot\frac{\Delta x^2}{6}\cos\Psi_p(z_w + 2y_w) - V_3\frac{z_w}{3}}{L_1\cos(\Psi_p + \Psi_T)} \quad \text{(For case 1)} \quad (37)$$

$$T_t = \frac{\frac{W_1(y_1\sin\Psi_p - \Delta x\cos\Psi_p)}{2} + P_1(y_1 - \Delta x\tan\phi_d) + V_1\frac{y_w}{3} + \gamma_w\cdot\frac{\Delta x^2}{6}\cos\Psi_p(y_w + z_w + (2i-1)\Delta x\sin\Psi_p) - V_3\frac{z_w}{3}}{L_1\cos(\Psi_p + \Psi_T)} \quad \text{(For case 2)} \quad (38)$$

$$T_t = \frac{\frac{W_1(y_1\sin\Psi_p - \Delta x\cos\Psi_p)}{2} + P_1(y_1 - \Delta x\tan\phi_d) + V_1\frac{y_w}{3} + \gamma_w\cdot\frac{\Delta x^2}{6}\cos\Psi_p(z_w + y_w + (2n-1)\Delta x\sin\Psi_p) - V_3\frac{z_w}{3}}{L_1\cos(\Psi_p + \Psi_T)} \quad \text{(For case3)} \quad (39)$$

$$T_s = \frac{P_1(1 - \tan\phi_p\tan\phi_d) - W_1(\tan\phi_p\cos\Psi_p - \sin\Psi_p) + V_1 - V_2\tan\phi_p - V_3}{\tan\phi_p\sin(\Psi_p + \Psi_T) + \cos(\Psi_p + \Psi_T)} \quad (40)$$

When T force is applied to block 1, the normal and shear force on the base of the block are respectively,

$$R_n = W_n\cos\Psi_p + (P_n - P_{n-1})\tan\phi_d + (V_1 - V_3)\tan\phi_d + -V_2\cos\Psi_p + T\sin(\Psi_T + \Psi_p), \quad (41)$$

$$S_n = W_n\sin\Psi_p + (P_n - P_{n-1}) - (V_1 - V_3) + -V_2\sin\Psi_p - T\cos(\Psi_T + \Psi_p). \quad (42)$$

6. Illustrative Example-1

Following is an example to describe the application of presented study to calculate inter column forces and factor of safety of rock slope susceptible to toppling failure and required anchoring force to stabilize the rock slope under the consideration of different hydraulic distribution forms. The example considered in this study has been taken from Wyllie and Mah (2004) shown in Fig. 10 and value of parameters of rock slope geometry as given in Table 1. Wyllie and Mah (2004) analysed the stability of rock slope considering dry slope.

Every block is stepped of 1 m height in its base from toe upwards. Therefore, Overall dip of failure plane along base Ψ_b is found to be (Ψ_p + tan (1/10)) 35.7°. Number. of block are calculated as 16 using Eq. (2) and rock block 10 is at the crest of slope

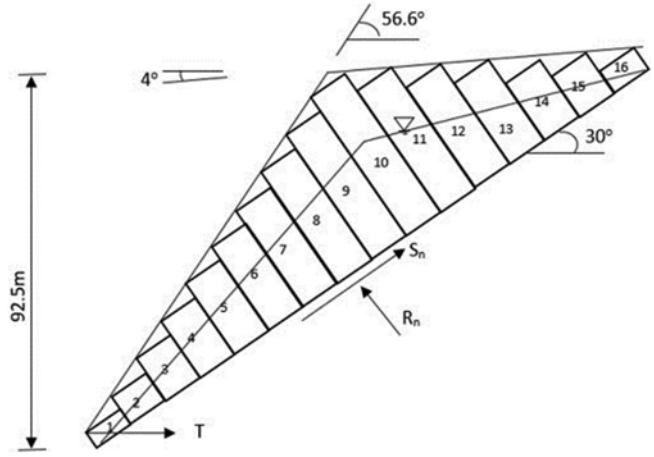

Fig. 10. Slope Geometry Representing Number of Blocks and Slope Parameters

Table 1. Slope Geometry Parameters and Rock Properties

Parameter	Symbol	Value
Height of slope (m)	H	92.5
Angle of slope face (Degree)	Ψ_f	56.6°
Dip of rock layers into slope face (Degree)	Ψ_d	60°
Angle of failure plane (Degree)	Ψ_p	30°
Width of block (m)	Δx	10
Angle of slope above crest (Degree)	Ψ_s	4°
Friction angle on the base of block (Degree)	ϕ_p	38.15°
Friction angle along the side of block (Degree)	ϕ_d	38.15°
Unit weight of rock (kN/m^3)	γ_r	25

(Fig. 10). Constant a_1, a_2 and b are found as 5.0 m, 5.2 m, 1.0 m using Eqs. (45), (46) and (47) respectively.

Table 2. Validation of Proposed Analytical Rock Slope Stability Model

Particulars	Wyllie and Mah (2004)	Present Study
Total no. of blocks	16	16
Force P_n at toe block	472.2	472.2
Force R_n at toe block	1237.1	1237.1
Force S_n at toe block	971.8	971.8
Critical mode	Sliding	Sliding
FS of slope	0.97	0.97

6.1 Validation of Proposed Rock Slope Stability Model

Developed stability model presented in this study is validated by comparing outcomes of special case i.e., dry slope condition with those of Wyllie and Mah (2004). For this special case, external forces i.e., ground water forces are assumed to be absent, or the slope considered to be dry. Input parameters as slope geometry and rock properties are same as Wyllie and Mah (2004) study shown in Table 1. Results of the developed model for dry slope conditions are found to be similar to Wyllie and Mah (2004) as shown in Table 2. This validates the proposed stability model and implies that it may be used for further stability analysis under the presence of external forces.

Limit equilibrium analysis of a rock slope under block toppling is performed using the input parameters as shown in Table 1, to assess the influence of the hydraulic forms on rock slope stability. Tables 3, 4 and 5 presents the inter column forces and failure mode of each block of rock slope for the cases (1), (2) and (3) respectively. Distribution of normal forces R_n and Shear forces S_n along the base of the blocks are shown in Figs. 11, 12, and 13 for rock slope under case (1), (2) and (3) respectively.

6.2 Illustrative Example 2

This example considered in the study has been taken from Bowa

Table 3. Results from the Limit Equilibrium Analysis of Slope for Case 1

n	y_n	M_n	L_n	z_w	y_w	$P_{n,t}$	$P_{n,s}$	P_n	R_n	S_n	S_n/R_n	Failure Mode
16	4	-	-	4	4	0	0	0	571.72	330.08	0.577346	Stable
15	10	5	10	10	10	0	0	0	1429.3	825.21	0.577353	
14	16	11	16	16	16	0	0	0	2018.1	978.08	0.484654	
13	22	17	22	22	22	342.25	-4670.9	342.25	2738.2	1298.2	0.474107	Toppling
12	28	23	28	20	22	859.51	-6080.3	859.51	4223.6	1520.7	0.360048	
11	34	29	34	18	20	1589.9	-5163.1	1589.9	5609.5	2346.9	0.41838	
10	40	35	35	16	18	2363.1	-4879	2363.1	6560.1	2618.8	0.399201	
9	36	36	31	14	16	3733.1	-4552.1	3733.1	5882.4	2324.2	0.395111	
8	32	32	27	13	14	5114.5	-1871.7	5114.5	5396.2	2511.3	0.465383	
7	28	28	23	11	13	5904.7	-704.18	5904.7	5047.6	2414.8	0.478406	
6	24	24	19	10	11	6265.4	1051	6265.4	4603.3	2604.3	0.565746	
5	20	20	15	8	10	6114.4	1844.4	6114.4	4273.3	2582.5	0.604334	
4	16	16	11	6	8	5484.3	2591.8	5484.3	3991.8	2799.2	0.701238	
3	12	12	7	4	6	4262.1	2692.2	4262.1	3819.3	3140.8	0.82235	
2	8	8	3	2	4	2308	2200.5	2308	2597	2152.7	0.828918	
1	4	4	-	0	2	-943.5	**976.9**	976.9	1555	1394.3	0.896656	Sliding

Table 4. Results from the Limit Equilibrium Analysis of Slope for Case 2

n	y_n	M_n	L_n	z_w	y_w	Pn,t	Pn,s	Pn,	Rn	Sn	Sn/Rn	Failure Mode
16	4	-	-	4	4	0	0	0	1647.2	1527.3	0.92721	Stable
15	10	5	10	10	10	0	0	0	736.38	326.97	0.444023	
14	16	11	16	16	16	179.64	-4226	179.64	1030	370.19	0.359408	Toppling
13	22	17	22	22	22	598.8	-6660	598.8	1391	479.47	0.344694	
12	28	23	28	20	22	1191.4	-8873	1191.4	2509	489.76	0.195201	
11	34	29	34	18	20	1997	-8752	1997	3527	1103	0.31273	
10	40	35	35	16	18	2845	-9263	2845	4047	1083.4	0.267704	
9	36	36	31	14	16	4370	-9733	4370	2900	447.28	0.154234	
8	32	32	27	13	14	5937	-8349	5937	1995	357.48	0.179188	
7	28	28	23	11	13	7086	-7287	7086	1217	30.267	0.02487	
6	24	24	19	10	11	7884	-6047	7884	326.02	153.6	0.471137	
5	20	20	15	8	10	8272	-5685	8272	-685	-522.48	0.762745	
4	16	16	11	6	8	8316	-5270	8316	-1282	-722.8	0.563807	
3	12	12	7	4	6	7968	-5366	7968	-2092.2	-922.83	0.441081	
2	8	8	3	2	4	7233	-5855	7233	-2922	-1163.2	0.398084	
1	4	4	-	0	2	6138	-6731	**6138**	-3256.1	-1489.4	0.457418	

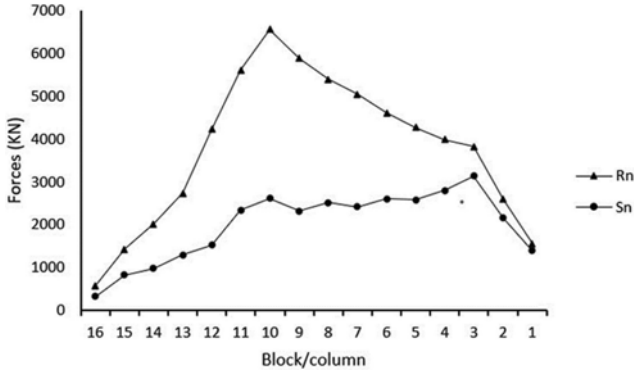

Fig. 11. Distribution of Normal Force R_n and Shear Force S_n along the Base of Blocks for Case 1

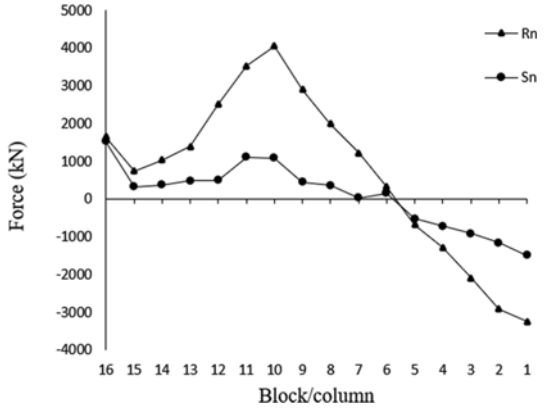

Fig. 12. Distribution of Normal Force R_n and Shear Force S_n along the Base of Blocks for Case 2

Table 5. Results from the Limit Equilibrium Analysis of Slope for Case 3

n	y_n	M_n	L_n	z_w	y_w	Pn,t	Pn,s	Pn,	Rn	Sn	Sn/Rn	Failure Mode
16	4	-	-	4	4	0	0	0	1647.2	1527.3	0.92721	Stable
15	10	5	10	10	10	0	0	0	736.38	326.97	0.444023	
14	16	11	16	16	16	179.64	-4226	179.64	1030	370.19	0.359408	Toppling
13	22	17	22	22	22	598.8	-6660	598.8	1391	479.4	0.344644	
12	28	23	28	20	22	1191.4	-8873	1191.4	2509	489.7	0.195177	
11	34	29	34	18	20	1997	-8752	1997	3527	1103	0.31273	
10	40	35	35	16	18	2845	-9263.9	2845	4047	1083.4	0.267704	
9	36	36	31	14	16	4370	-9733.5	4370	2900	447.28	0.154234	
8	32	32	27	13	14	5937	-8349	5937	2404.6	622.3	0.258796	
7	28	28	23	11	13	7033.6	-64146.2	7033.6	2460.7	785.09	0.319051	
6	24	24	19	10	11	7654.3	-3483.3	7654.3	2431	1246.5	0.512752	
5	20	20	15	8	10	7704.5	-1588.7	7704.5	2531.7	1517	0.599202	
4	16	16	11	6	8	7196.5	261.22	7196.5	2710.2	2056.4	0.758763	
3	12	12	7	4	6	5980.4	1355	5980.4	3065.5	2820.9	0.920209	
2	8	8	3	2	4	3831.2	1740.6	3831.2	3071.7	2978	0.969496	
1	4	4	-	0	2	-161.99	1193	1193	1435.8	1370.6	0.95459	Sliding

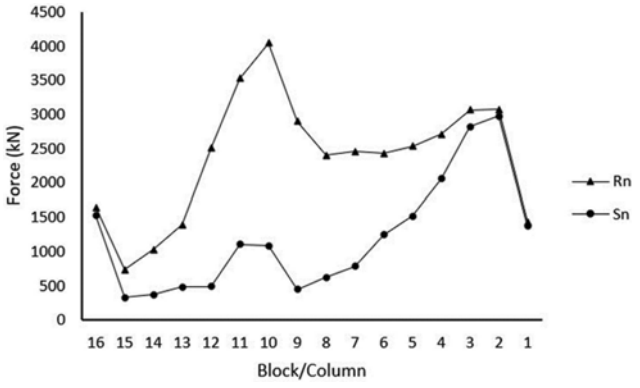

Fig. 13. Distribution of Normal Force R_n and Shear Force S_n along the Base of Blocks for Case 3

and Gong (2021) to conduct a comparative analysis, assessing the stability of a rock slope with respect to conventionally adopted hydraulic distribution form (similar to case 1) and other hydraulic distribution forms presented in this study. Considered slope is of 90 m height with slope face inclined at an angle 65°, and failure plane inclined at 35°. Unit weight of rock slope is 26 kN/m^3. Block width is 10 m. Internal angle of friction along the side and base of block is 30°.

Number of blocks are calculated using Eq. (2) and comes out to be 14. For the comparative stability analysis under different hydraulic forms, slope is considered as 50% wet slope. Limit equilibrium analysis to calculate Interblock force is performed. Interblock force and failure mode are calculated for each block. Forces at toe blocks are presented in Table 6.

7. Result and Discussion

In the absence of external forces, kinematic conditions for block toppling are checked before proceeding to the main stability (kinetic) analysis to determine whether the overall mechanism is favourable to toppling or not. In the presented study, Ground water is considered as an external force, and the stability of rock slope subject to block toppling is evaluated considering three different hydraulic forms according to various field conditions. Here, kinetic stability is evaluated using limit equilibrium method, which involves a process in which geometry of all blocks is calculated, followed by determination of inter-block forces. Subsequently, stability of each block is examined starting with the uppermost block. Each block will be either stable, toppling or sliding.

Considering Example 1, In a case 1 when it is assumed that maximum water pressure is at the base of the block, Stability analysis outcomes of rock slope subjected to block toppling are listed in Table 3. It can be observed from Table 3 that blocks 16, 15 and 14 are stable. P_{13} is calculated as greater of $P_{13,t}$ and $P_{13,s}$ given by Eqs. (18) and (19) respectively. This calculation approach is used to examine the stability of each block as it proceeds down the slope. $P_{n\text{-}1,t}$ is greater than $P_{n\text{-}1,s}$ until block 2. Thus block 13 to 2 forms the potential toppling zone. Block 1 constituents a sliding zone whereupon $P_{n\text{-}1,s}$ is greater than $P_{n\text{-}1,t}$. Factor of this slope is calculated by increasing the friction angle in small increments until the toe block are just stable. It is observed that required friction angle for limit equilibrium condition is found to be 39°. Thus, the factor of safety using Eq. (14) is 0.97. Required tension in an anchor installed at an angle 25° in block 1 just to stabilise the toe block is 1,200 kN per meter length of slope. Normal forces R_n and Shear forces S_n on the base of blocks are obtained using Eqs. (20) and (21) respectively. Fig. 11 shows the distribution of normal force R_n and Shear force S_n along the base of block throughout the slope. Condition $R_n > 0$ & $|S_n| < R_n \tan\phi_p$ are satisfied for every block. This criterion indicates that blocks do not slide along the base.

In a case 2, when water pressure is assumed to be maximum at toe of rock slope due to the blockage of flow slit. Limit equilibrium analysis to calculate Interblock force is performed (Table 4). Interblock force and failure mode are calculated for each block, and it can be observed, block 16, 15 are stable and block 14 to toe block are observed to be fail in toppling. Unlike case 1, here toe block fails in toppling and has toppling force appx 6,138 kN i.e., appx six times to case 1. It can be interpreted as in the case of blockage of flow in rock slope increases the toppling tendency of blocks. Required friction angle for the calculation of factor of safety is 52.8° and factor of safety using Eq. (14) is 0.59. Anchor force required to stabilise the toe block is 8,500 kN required to install at an angle 25° i.e., almost 7 times more anchore force is required in comparison to case 1. Fig. 12 shows the distribution of normal force R_n and Shear force S_n along the base of block throughout the slope. Condition $R_n > 0$ & $|S_n| < R_n \tan\phi_p$ are satisfied for blocks above block 5. it indicates that sliding can also occur on the base of blocks from block 5 to toe block.

In a case 3, when water pressure is assumed to be maximum

Table 6. Results of Stability Analysis of Rock Slope under Different Hydraulic Distribution Forms

Particulars	Bowa and Gong (2021)				Present Study			
	Force P_n at toe block (kN)	Force R_n at toe block (kN)	Force S_n at toe block (kN)	Critical mode	Force P_n at toe block (kN)	Force R_n at toe block (kN)	Force S_n at toe block (kN)	Critical mode
Dry Slope	-9.6	666.3	355.3	Sliding	-9.6	666.3	355.3	Sliding
Case 1	127.8	1951.4	1736.3	Sliding	127.8	1951.4	1736.3	Sliding
Case 2	-	-	-	-	749.2	3946.3	1739.8	Sliding
Case 3	-	-	-	-	154.9	1765.4	1368.9	Sliding

at half distance along the base of slope. Outcomes of limit equilibrium analysis of block toppling are listed in Table 5. It is observed that blocks 15 and 16 are stable. $P_{n\text{-}1,\,t}$ is greater than $P_{n\text{-}1,\,s}$ for block 14 to 2, thus forms a toppling zone. Similar to case (1), here toe block constituents a sliding zone as $P_{n\text{-}1,\,s}$ is greater than $P_{n\text{-}1,\,t}$. Required friction angle for the limit equilibrium condition is found to be 40.8°. Thus, factor of safety for rock slope under case 3 is 0.91. Required tension in an anchor installed at an angle 25° in block 1 just to stabilise the toe block is 1,850 kN per meter length of slope. Considering hydraulic distribution as per case 3, factor of safety, force at toe and anchor force is much close to case1, and significantly lesser than case 2. Condition $R_n > 0$ & $|S_n| < R_n \tan\phi_p$ are satisfied for every block It simply implies no block slides along the base of the block.

In the context of example 2, Under dry condition and case 1, when it is assumed that maximum water pressure is at the base of the block, Stability analysis outcomes of rock slope subjected to block toppling are similar to outcomes presented by (Bowa and Gong, 2021). This alignment substantiates the validity of the proposed stability model, suggesting its applicability for comprehensive stability analyses under different hydraulic conditions. Sliding Force at toe block under case 2 indicating blocked flow condition at slit is appx. Sixfold increase compared to case 1 aligning with the trend observed in Example 1. Moving on to case 3, outcomes closely resembles those of case 1.

Presence of water in discontinuities or vertical fissures increases slope instability by reducing the shear strength of potential failure surface. It is also being observed that due to the variation in ground water level in some rock formations can accelerate weathering and reduces shear strength. Consequently, affects slope stability (Zhao et al., 2015). While investigating a rock slope, it is possible to make the misconception of assuming that ground water does not exist if there is no seepage of water on the slope face. The seepage rate could be lower, and the slope surface may seem dry. Due to the partial or full blockage of flow, there may be water at high pressure within the rock mass. Water pressure is majorly responsible for instability in slopes, not the rate of flow of water and it is absolutely essential that assessment of water depth and estimation of water pressure form an important part of site investigations for stability analysis.

8. Conclusions

In this study, an analytical solution using limit equilibrium approach for block toppling failure under different hydraulic forms is proposed. In this analysis, ground water pressure is considered as an external force, and three different hydraulic distribution forms are explored based on various water flow conditions through slip at toe of rock slope, which have been overlooked in the available literature. It is a well-known fact that presence of ground water affects the stability of slope. It is observed from this study that hydraulic distribution forms have a significant impact on the stability of rock slopes. Furthermore, it has also been noted that presence of ground water significantly increases the toppling forces on the blocks. The increase in toppling force on the blocks is more prominent when the flow slit is blocked (Case 2), indicating a condition of permanent or seasonal frozen strata. The toppling force at toe block in case 2 is much higher (appx. six folds) than force calculated from traditionally adopted hydraulic distribution form (case 1). The study underscores the importance of considering water pressure in rock mass, even in the absence of visible seepage, as it plays a pivotal role in slope instability. The findings emphasize the necessity of assessing water depth and estimating water pressure in site investigations to comprehensively address slope stability concerns. It can be concluded that just adopting traditional hydraulic form to analyse the rock slope susceptible to block toppling considering presence of ground water, would not be appropriate for all field conditions. This necessitates the selection of suitable hydraulic distribution form based on the encountered field condition. The study also shows that ground water reduces the normal and shear force on the base of blocks, thereby inducing failure of rock slope subjected to block toppling.

Acknowledgments

This research did not receive any specific grant from funding agencies in the public, commercial, or not-for-profit sectors.

Nomenclature

a_1 = Height difference at the top of adjacent blocks below the crest
a_2 = Height difference at the top of adjacent blocks above the crest
b = The height difference at the base of adjacent blocks
H = Slope Height
L_n = Distance from the base of the block to the point of application of $P_{n\text{-}1}$
M_n = Distance from the base of the block to the point of application of P_n
N = Total number of blocks
n = Number of block (numbered from toe to uppermost block)
P_n = The normal force of n + 1th block to nth block
$P_{n\text{-}1}$ = The normal force of n - 1th block to nth block
Q_n = Shear force between n + 1th and nth block
$Q_{n\text{-}1}$ = Shear force between n - 1th and nth block
R_n = Normal force at the base of nth block
S_n = Shear force along the base of nth block
V_1, V_3 = Ground water forces along the sides of block
V_2 = Ground water forces along the base of block
W_n = Weight of nth block
y_n = Height of nth block
y_w, z_w = Depth of the water along the sides of block
α_a = Dip direction of discontinuity along base
α_b = Dip direction of discontinuity along width
α_s = Dip direction of discontinuity along face
Δx = Width of block

γ_r = Unit weight of rock
γ_w = Unit weight of water
ϕ_b = Overall dip of failure plane along base
ϕ_d = Friction angle along the side of the block
ϕ_p = Friction angle along the base of the block
Ψ_d = Dip of the orthogonal plans forming the sides of the blocks
Ψ_f = Slope angle below the crest
Ψ_p = Dip of plane forming base of the block
Ψ_s = Slope angle above the crest

ORCID

Not Applicable

References

Adhikary DP, Dyskin Av, Jewell RJ, Stewart DP (1997) A study of the mechanism of flexural toppling failure of rock slopes. *Rock Mechanics and Rock Engineering* 30(2):75-93, DOI: 10.1007/BF01020126

Alejano LR, Sánchez-Alonso C, Pérez-Rey I, Arzúa J, Alonso E, González J, Beltramone L, Ferrero AM (2018) Block toppling stability in the case of rock blocks with rounded edges. *Engineering Geology* 234:192-203, DOI: 10.1016/j.enggeo.2018.01.010

Amini M, Ardestani A, Khosravi MH (2017) Stability analysis of slide-toe-toppling failure. *Engineering Geology* 228:82-96, DOI: 10.1016/j.enggeo.2017.07.008

Ashby J (1971) Sliding and toppling modes of failure in models and jointed rock slopes. Imperial College, University of London

Aydan, Kawamoto T (1992) The stability of slopes and underground openings against flexural toppling and their stabilisation. *Rock Mechanics and Rock Engineering* 25(3):143-165, DOI: 10.1007/BF01019709

Azarafza M, Asghari-Kaljahi E, Ghazifard A, Akgün H (2021) Application of fuzzy expert decision-making system for rock slope block-toppling modeling and assessment: A case study. *Modeling Earth Systems and Environment* 7(1):159-168, DOI: 10.1007/s40808-020-00877-9

Bobet A (1999) Analytical solutions for toppling failure. *International Journal of Rock Mechanics and Mining Sciences* 36(7):971-980, DOI: 10.1016/S0148-9062(99)00059-5

Bowa VM, Gong W (2021) Analytical technique for stability analyses of the rock slope subjected to slide head toppling failure mechanisms considering groundwater and stabilization effects. *International Journal of Geo-Engineering* 12(1), DOI: 10.1186/s40703-020-00133-0

Bowa VM, Xia Y (2018) Stability analyses of jointed rock slopes with counter-tilted failure surface subjected to block toppling failure mechanisms. *Arabian Journal for Science and Engineering* 43(10):5315-5331, DOI: 10.1007/s13369-018-3168-4

Chen Z, Wang X, Yang J, Jia Z, Wang Y (2005) Rock slope stability analysis-theory, methods and programs. China Water & Power Press: Bejing, China

Cruden DM (1989) Limits to common toppling. *Canadian Geotechnical Journal* 26(4):737-742

Goodman RE, Bray JW (1976) Toppling of rock slopes. *Proceedings of the Specialty Conference on Rock Engineering for Foundations and Slopes* 2:201-234

Hoek E, Bray JD (1981) Rock slope engineering. CRC Press, DOI: 10.1201/9781482267099

Liu CH, Jaksa MB, Meyers AG (2008) Improved analytical solution for toppling stability analysis of rock slopes. *International Journal of Rock Mechanics and Mining Sciences* 45(8):1361-1372, DOI: 10.1016/j.ijrmms.2008.01.009

Luo Q, Li L, Zhao LH (2010) Quasi-static analysis on the seismic stability of anchored rock slope with the effect of surcharge and water pressure conditions. *Rock and Soil Mechanics* 31:3585-3593

Muller L (1968) New consideration on the vaiont slide. *Rock Mechanics and Engineering Geology* 6:1-91

Roy D, Maheshwari P (2018) Probabilistic analysis of rock slopes against block toppling failure. *Indian Geotechnical Journal* 48(3):484-497, DOI: 10.1007/s40098-017-0281-3

Sagaseta C, Ca J (2001) A general analytical solution for the required anchor force in rock slopes with toppling failure. *International Journal of Rock Mechanics & Mining Sciences,* 38

Samadi M, Sarkardeh H, Jabbari E (2020) Explicit data-driven models for prediction of pressure fluctuations occur during turbulent flows on sloping channels. *Stochastic Environmental Research and Risk Assessment* 34(5):691-707, DOI: 10.1007/s00477-020-01794-0

Samadi M, Sarkardeh H, Jabbari E (2021) Prediction of the dynamic pressure distribution in hydraulic structures using soft computing methods. *Soft Computing* 25(5):3873-3888, DOI: 10.1007/s00500-020-05413-6

Sari M (2019) Stability analysis of cut slopes using empirical, kinematical, numerical and limit equilibrium methods: Case of old Jeddah–Mecca road (Saudi Arabia). *Environmental Earth Sciences* 78(21):621, DOI: 10.1007/s12665-019-8573-9

Shafagh Loron R, Samadi M, Shamsai A (2023) Predictive explicit expressions from data-driven models for estimation of scour depth below ski-jump bucket spillways. *Water Supply* 23(1):304-316, DOI: 10.2166/ws.2022.421

Shu JS, Wang XZ, Zhou YY (2004) Improving on assumption for water pressure distributing on failure surface in rock slope. *Journal of China University of Mining and Technology* 33:509-512

Tang HM, Chen HK (2008) Revised method of water pressure in control fissure of perilous rockmass. *The Chinese Journal of Geological Hazard and Control* 19:86-90

Tatone BSA, Grasselli G (2010) ROCKTOPPLE: A spreadsheet-based program for probabilistic block-toppling analysis. *Computers and Geosciences* 36(1):98-114, DOI: 10.1016/j.cageo.2009.04.014

Willey DC (1980) Toppling rock slope failures examples of analysis and stabilization. *Rock Mechanics*, 13

Wyllie DC, Mah CW (2004) Rock slope engineering civil and mining. In: Hoek, E. and Bray, J.W., Eds., Rock slope Engineering, Taylor & Francis Group, London and New York, 431

Wyllie DC, Mah CW (2017) Rock slope engineering. Fourth Edition CRC Press, DOI: 10.1201/9781315274980

Yagoda-Biran G, Hatzor YH (2013) A new failure mode chart for toppling and sliding with consideration of earthquake inertia force. *International Journal of Rock Mechanics and Mining Sciences* 64:122-131, DOI: 10.1016/j.ijrmms.2013.08.035

Zanbak C (1983) Design charts for rock slopes susceptible to toppling. *Journal of Geotechnical Engineering* 109(8):1039-1062, DOI: 10.1061/(ASCE)0733-9410(1983)109:8(1039)

Zhang Z, Wang T, Wu S, Tang H (2016) Rock toppling failure mode influenced by local response to earthquakes. *Bulletin of Engineering Geology and the Environment* 75(4):1361-1375, DOI: 10.1007/s10064-015-0806-x

Zhao LH, Cao J, Zhang Y, Luo Q (2015) Effect of hydraulic distribution on the stability of a plane slide rock slope under the nonlinear

Barton-Bandis failure criterion. *Geomechanics and Engineering*, 8(3):391-414, DOI: 10.12989/gae.2015.8.3.391

Zhao LH, Luo Q, Li L, Dan HC, Luo SP (2011) Stability of subgrade slope along river subjected to water level fluctuations and stream erosion. *Journal of Highway and Transportation Research and Development* 5(2):1-9

Zheng Y, Chen C-X, Zhu X-X, Ou Z, Liu X-M, Liu T (2014) Analysis of toppling failure of rock slopes subjected to seismic loads. *Rock and Soil Mechanics* 35(4):1025-1032

Appendix A

Procedure to Calculate the Geometric Parameters (Goodman and Bray, 1976)

Block are numbered from toe block upwards. Height y_n for block below and above the crest is given by Eqs. (43) and (44) respectively.

$$y_n = n(a_1 - b) \tag{43}$$

$$y_n = y_{n-1} - a_2 - b \tag{44}$$

Constants a_1, a_2, and b can be computed by resolving slope and block geometry as given in Eqs. (45), (46) and (47)

$$a_1 = \Delta x \tan(\Psi_f - \Psi_p), \tag{45}$$

$$a_2 = \Delta x \tan(\Psi_p - \Psi_s), \tag{46}$$

$$b = \Delta x \tan(\Psi_b - \Psi_p) \tag{47}$$

To conduct stability analysis, point of application of normal forces i.e., M_n and Ln (Fig. 2) on the upper and lower faces of block respectively are required, and are given by the following set of equations

If nth block is below the slope crest,

$$M_n = y_n, \tag{48}$$

$$L_n = y_n - a_1. \tag{49}$$

If nth block is at slope crest,

$$M_n = y_n - a_2, \tag{50}$$

$$L_n = y_n - a_1. \tag{51}$$

If nth block is below the slope crest,

$$M_n = y_n - a_2, \tag{52}$$

$$L_n = y_n. \tag{53}$$

Appendix B

Number of Blocks Forming the System

Figure 14 shows a schematic diagram of rock slope illustrating basic slope geometrical parameters. In the calculation of slope geometry and stability analysis, width of all the block is considered to be same. If upper slope is not present, $\Psi_s = 0$

$$n = \frac{H \operatorname{cosc} \Psi_b}{\Delta x} \tag{54}$$

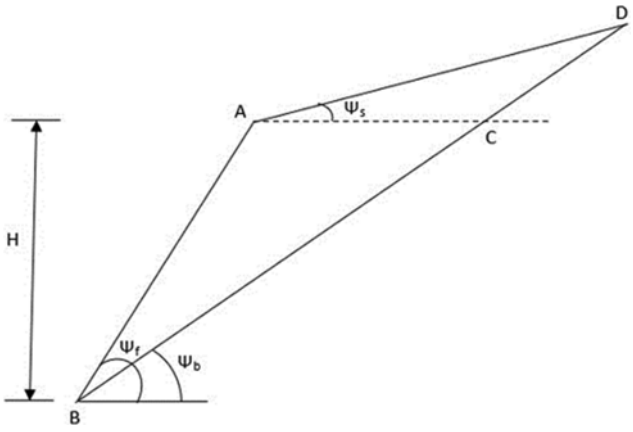

Fig. 14. Slope Geometry Showing Basic Slope Parameters

In the considered geometry, $\Psi_s \neq 0$

$$AC = H \cot \Psi_b - H \cot \Psi_f. \tag{55}$$

In ΔADC

$$\frac{AC}{\sin(\Psi_b - \Psi_s)} = \frac{CD}{\sin \Psi_s}, \tag{56}$$

$$CD = \frac{H(\cot \Psi_b - \cos \Psi_f)\sin \Psi_s}{\sin(\Psi_b - \Psi_s)}. \tag{57}$$

No. of blocks,

$$n = \frac{BC + CD}{\Delta x}, \tag{58}$$

$$n = \frac{H}{\Delta x}\left(\operatorname{cosec} \Psi_b + \frac{(\cot \Psi_b - \cot \Psi_f)\sin \Psi_s}{\sin(\Psi_b - \Psi_s)}\right). \tag{59}$$

Appendix C

Limit Equilibrium for Toppling of nth Block

Considering rotational equilibrium, net moment of point O is zero

$$\sum M_o = 0, \tag{60}$$

$$P_n M_n + W_n \sin \Psi_p \frac{y_n}{2} - W_n \cos \Psi_p \frac{\Delta x}{2} - Q_n \Delta x - P_{n-1,t} L_n = 0. \tag{61}$$

Substituting the value of Q_n from Eq. (7) and rearranging,

$$P_{n-1,t} L_n = P_n M_n + W_n \sin \Psi_p \frac{y_n}{2} - W_n \cos \Psi_p \frac{\Delta x}{2} - P_n \tan \phi_d \Delta x. \tag{62}$$

Therefore, toppling force is obtained as

$$P_{n-1,t} = \frac{P_n(M_n - \Delta x \tan \phi_d) + \left(\frac{W_n}{2}\right)(y_n \sin \Psi_p - \Delta x \cos \Psi_p)}{L_n}. \tag{63}$$

Appendix D

Limit Equilibrium for Sliding of nth Block

Resolving force in the direction of $P_{n\text{-}1}$

$$P_{n-1,s} - P_n + R_n \tan\phi_p - W_n \sin\Psi_p = 0 . \quad (63)$$

Forces in the direction of perpendicular to $P_{n\text{-}1}$

$$R_n = W_n \cos\Psi_p + (P_n - P_{n-1,s})\tan\phi_d . \quad (64)$$

Substitute value of R_n in Eq. (63)

$$P_{n-1,s} - P_n + [W_n \cos\Psi_p + (P_n - P_{n-1,s})\tan\phi_d]\tan\phi_p - W_n \cos\Psi_p = 0 . \quad (65)$$

This can be rewritten as

$$\begin{aligned} &P_{n-1,s}(1 - \tan\phi_d \tan\phi_p) - P_n(1 - \tan\phi_d \tan\phi_p) \\ &W_n(\cos\Psi_p \tan\phi_p - \sin\Psi_p) = 0 \end{aligned} . \quad (66)$$

Therefore, Eq. of sliding force is obtained as

$$P_{n-1,s} = P_n - \frac{W_n(\cos\Psi_p \tan\phi_p - \sin\Psi_p)}{(1 - \tan\phi_p \tan\phi_d)} . \quad (67)$$